



The role of Holocene climate dynamics in the modeling of fluviomarine terraces in the northeastern Brazilian coast



Vinicius Borges Moreira ^{a,*} , Luca Lämmle ^{b,c} , Mariarca D'Aniello ^{d,e}, Fabiano Tomazini Da Conceição ^a , Carlo Donadio ^{d,f} , Archimedes Perez Filho ^b

^a Institute of Geosciences and Exact Sciences, São Paulo State University (UNESP), Av. 24 A 1515, 13506-700, Rio Claro, Brazil

^b Department of Geography, Institute of Geosciences, University of Campinas (UNICAMP), Via Carlos Gomes 250, 13083-855, Campinas, Brazil

^c Department of Geology, University of Patras, Rio-Patras, GR-26504, Greece

^d Department of Earth Sciences, Environment and Resources, University of Naples Federico II, University Campus of Monte Sant'Angelo, Via Vicinale Cupa Cintia 21, 80126, Napoli, Italy

^e National Institute for Astrophysics, INAF-OAC, Salita Moiariello, 16, 80131, Napoli, Italy

^f Stazione Zoologica Anton Dohrn, Villa Comunale, 80122, Napoli, Italy

ARTICLE INFO

Keywords:

Coastal geomorphology
Transitional environment
Fluviomarine terrace
OSL dating
Brazil

ABSTRACT

Fluviomarine terraces comprise mixed sedimentary sequences formed through the interplay of fluvial and marine aggradational morphodynamics. Although they are very common along the vast Brazilian coast, they are currently little explored in the geomorphological literature. In recent official mappings, it is common to observe the classification of the last or predominant event in each sector of the plain, with the discussion of fluviomarine morphologies being little explored. Therefore, this study aims to analyze transitional environments near the Rio Pardo River estuary, located on the northeastern Brazilian coast, within the alluvial-coastal system, which presents complex morphosedimentary archives consolidated during the regressive trend of the Holocene Relative Sea Level. To better understand the genesis, chronology, and vertical sequence that formed these fluviomarine terraces. A morphological description of three stratigraphic profiles exposed on erosive riverbanks was conducted using optically stimulated luminescence dating, sediment grain size characterization, and environmental depositional conditions and pedogenesis process. The results suggest five distinct depositional stages occurred, driven by Holocene climatic variations in the region with close correlation with Bond events and variations of the Intertropical Convergence Zone and South Atlantic Convergence Zone: 1 - Early Holocene $\sim 10.59 \pm 0.85$ ka; 2 - Middle Holocene $\sim 5.30 \pm 0.66$ ka and 4.57 ± 0.48 ka; 3 - Late Holocene A $\sim 3.44 \pm 0.31$ ka; 4 - Late Holocene B ~ 2.5 ka; 5 - Modern surface deposits $\sim 1.93 \pm 0.20$; 1.59 ± 0.18 and 1.46 ± 0.1 ka. Thus, the fluviomarine terraces analyzed constituted support for the identification of the climatic pulses that occurred in the Holocene along the Brazilian northeast coast.

1. Introduction

Studies related to spatial distribution and interpretation of morphogenesis have been carried out in Brazil since the 1950s, pioneered investigations by Silveira (1952), Ab'Sáber (1955), and Tricart (1958), who identified different types and levels of terraces in various regions of the extensive Brazilian coast. These authors introduced the term "fluviomarine terrace" into the scientific literature, which is applied here and consists of deposits of mixed origin (fluvial and marine) occurring intercalated in different sectors of a coastal plain, influenced by oscillations in marine and fluvial dynamics at different scales (Souza

et al., 2024). Such morphologies are commonly found near meandering rivers, paleochannels, lakes and lagoons consolidated or extinct during the regressive trend of the Brazilian coast during the Holocene, generating complex units, especially in estuarine and deltas (Laprida et al., 2007; Godiva et al., 2010; Arruda et al., 2023; Ribeiro et al., 2023; Barra et al., 2024), different from those of other geomorphic systems (Pennetta et al., 2016; Aiello et al., 2018; Donadio et al., 2018).

In addition, they are fundamental in paleogeographic reconstructions, providing support for the identification of different eustatic events related to phases of Relative Sea Level (RSL) advance and recovery, which may be associated with Holocene climate variations or

* Corresponding author.

E-mail address: vinicius.moreira@unesp.br (V.B. Moreira).

local factors (Suguio, 2010). This study suggests that fluviomarine terraces have erosional and depositional records correlated with regressive marine deposits, modeled at different levels (Moreira et al., 2024). Therefore, they can be an alternative or complementary environmental indicator to understand the coastal morphodynamics of the Brazilian northeastern coast.

Several studies have demonstrated the importance of sea level fluctuations and coastline displacements associated with climate dynamics during the Quaternary, illustrating the complex evolution of these transitional environments (Lauff, 1967; Buso Junior et al., 2013; De Miranda et al., 2017; Dillenburg et al., 2017; Mann et al., 2023; Rovere et al., 2023; Georgiou et al., 2024). Lauff (1967) and Schubel (1971) describe how all modern estuaries were formed during the most recent RSL elevations, and today it is possible to find estuaries around the world in various stages of this evolutionary process. The last RSL elevation that affected the entire Brazilian coast occurred ~6 ka ago (Angulo et al., 2006), but near the study area, more modern elevations of the RSL were evidenced, as well as different periods of coastal progradation Moreira et al. (2024). Thus, the climate and its variation during the Holocene can be considered one of the main factors influencing this dynamic (Arnaud-Fassetta, 2003; Masselink et al., 2011).

Here, we characterize and interpret the different layers of sedimentary deposits that make up fluviomarine terraces outcropping in the northeastern region of the Brazilian coast, through their spatialization, grain-size and sedimentological analysis, and ages by optically stimulated luminescence (OSL), associating them with the variations of the local RSL, climate and fluvial dynamics. Furthermore, we aim to consolidate the concept of fluviomarine terraces in geomorphological literature, making it accessible to the international community, as is the case with the concepts of fluvial terraces and marine terraces. In this sense, we adopted a specific approach to analyze these geomorphic

units, demonstrating their importance in the paleoenvironmental interpretation of estuarine environments and revisiting this concept in the current scientific debate.

2. Study area

The study area is located on the east coast of Brazil, specifically in the northeast region (Fig. 1). It consists of an estuarine system located north of the Jequitinhonha River delta, a region known as Cacau coast, south of the state of Bahia (Nascimento et al., 2007). This area exhibits a distinct morphological pattern, separate from traditional estuaries, where multiple river channels from different hydrographic basins converge at a single outlet, protected by barrier islands seaward. Additionally, unlike the most common river outlet on the Brazilian coast (Lämmle et al., 2022a,b; Dominguez et al., 2023a,b), the rivers on the Cacau coast show abrupt sinuosity close to the current coastline, with the river channel converging to the North or South at an angle of approximately 90°, causing it to reach parallel to the current shore (Fig. 1), similarly to other world coastal-alluvial plains as in the Mediterranean Basin where tilting due to volcano-tectonics and recent subsidence occurred in the Late Pleistocene-Holocene (De Pippo et al., 2001, 2000; Barra et al., 2024). Another regional coastal characteristic is the occurrence of abandoned paleochannels and scars from river captures, as well as connections between the different hydrographic basins through secondary channels, demonstrating intense interaction between rivers and their basins in this sector (Moreira et al., 2024).

Climatically, the study area is classified as type Af in the Köppen classification (Köppen, 1936; Kottek et al., 2006), characterized by a humid tropical climate. The highest rainfall is concentrated from March to August, with no distinct dry season. The tidal range, especially on the coast adjacent to the Pardo River and Jequitinhonha, is 1.73 m.

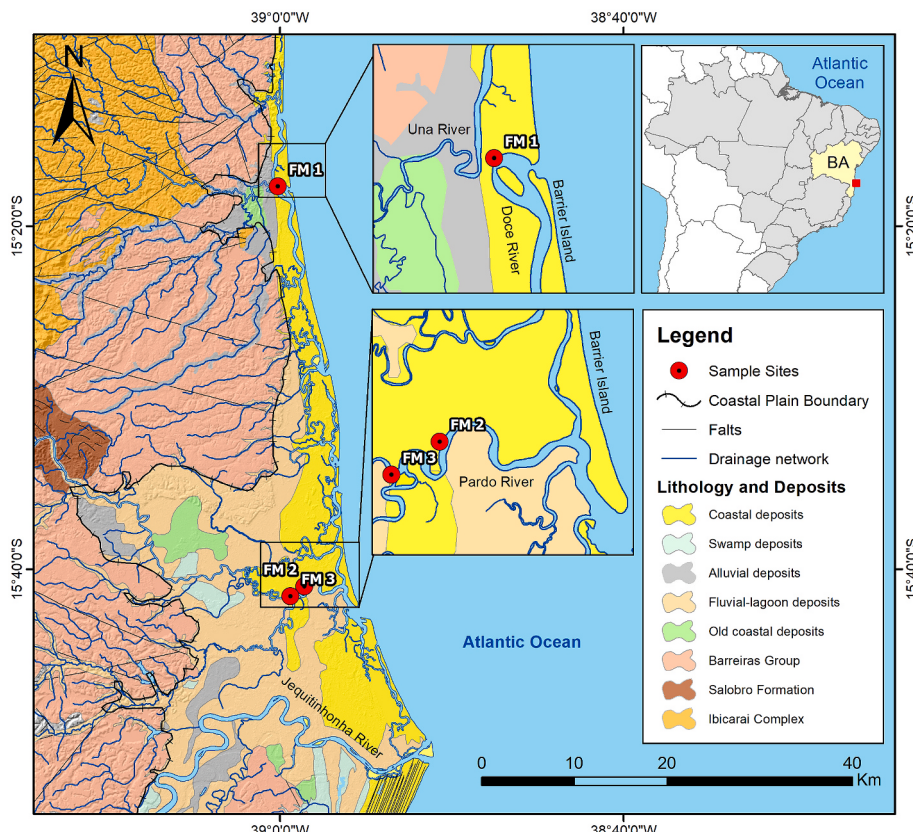


Fig. 1. – Study area, with location of sampled sites (FM1, FM2, and FM3), highlighting the main lithologies and sedimentary deposits. Source: CPRM - Companhia de Pesquisa de Recursos Minerais, 2006; CPRM - Companhia de Pesquisa de Recursos Minerais, 2010. Adapted by the authors. The geographic coordinate system is WGS 1984.

(Dominguez, 2023). In terms of lithology and predominant deposits aspects (Fig. 1), the Ibicaraí Complex, the Salobro Formation, and the Barreiras Group, the last forming the basis for structuring the relief of the coastal plateau in southern Bahia, represent the internal limit of the coastal plain. According to Araújo et al. (2006), the Barreiras Group is the most significant geological unit in Brazil, occurring from the north of Rio de Janeiro to the state of Amapá along the Brazilian coast. It is characterized by sediments and paleosols with facies of variable granulometry. According to Monteiro et al. (2022), the sediments of the Barreiras Group were deposited between 26 and 20 Ma, later being eroded and shaped by the various Quaternary marine transgressions that established the internal limits of the current coastal plain (Dominguez, 1982).

From the Late Pleistocene onwards, the coastal deposits were formed during different moments of RSL variation, but with a significant regressive trend from the middle Holocene onwards (Martin et al., 2003; Angulo et al., 2006). Moreira et al. (2024) describe these phases, differentiating the marine deposits topographically and chronologically, and highlighting the various levels of marine terraces present in the region, which enables the construction of an evolutionary reference model. Fluvimarine terraces occur in transitional areas between alluvial swamp and mangrove deposits, fluvio-lagoon, and coastal deposits in the study area and were not mapped by CPRM (2006). Examples of fluvimarine terraces characterized here were observed on the erosive banks of meandering rivers, which exposed the distinct layers of the mixed deposits analyzed (Fig. 2).

3. Materials and methods

3.1. Site identification and sampling

To identify the occurrence of fluvimarine terraces, cartographic materials (CPRM, 2006, 2010) and research and mapping techniques pioneered by Bacoccoli (1971), Martin et al. (1980), Dominguez et al. (1982), and Martin et al. (1993) were utilized. Additionally, information was obtained from the results of the morphometric parameters applied by Moreira (2021) and Moreira et al. (2024). We also utilized the Shuttle Radar Topography Mission 2 (SRTM2) digital elevation model (DEM) with a spatial resolution of 30 m, available at USGS Earth Explorer (<https://earthexplorer.usgs.gov/>) (accessed September 18, 2024), and images from Google Earth Pro (<https://www.google.com.br/earth/>) (accessed January 10, 2025).

In the field work, several surveys were carried out in the study area via local roads and boat along the main rivers in the region, as there are few bridges crossing the rivers and many flooded areas, which made access difficult. In this way, the profiles exposed on the erosive river-banks were identified and photographed for a macromorphological description of the stratigraphic columns and collection of samples for analysis. The sedimentary profile FM1 was collected on the erosive bank of the Doce River (Fig. 2a and c), which flows parallel to the coastline bordering the barrier island. The other two sedimentary profiles were collected on erosive banks of the Pardo River, with FM2 and FM3 sampled on the left bank (Fig. 2b, d, and 2e) and at the junction of the Pardo River with the Salsa River (Fig. 2b and f), respectively.

3.2. Stratigraphic columns and grain-size analysis

Stratigraphic columns were created to represent and systematize the

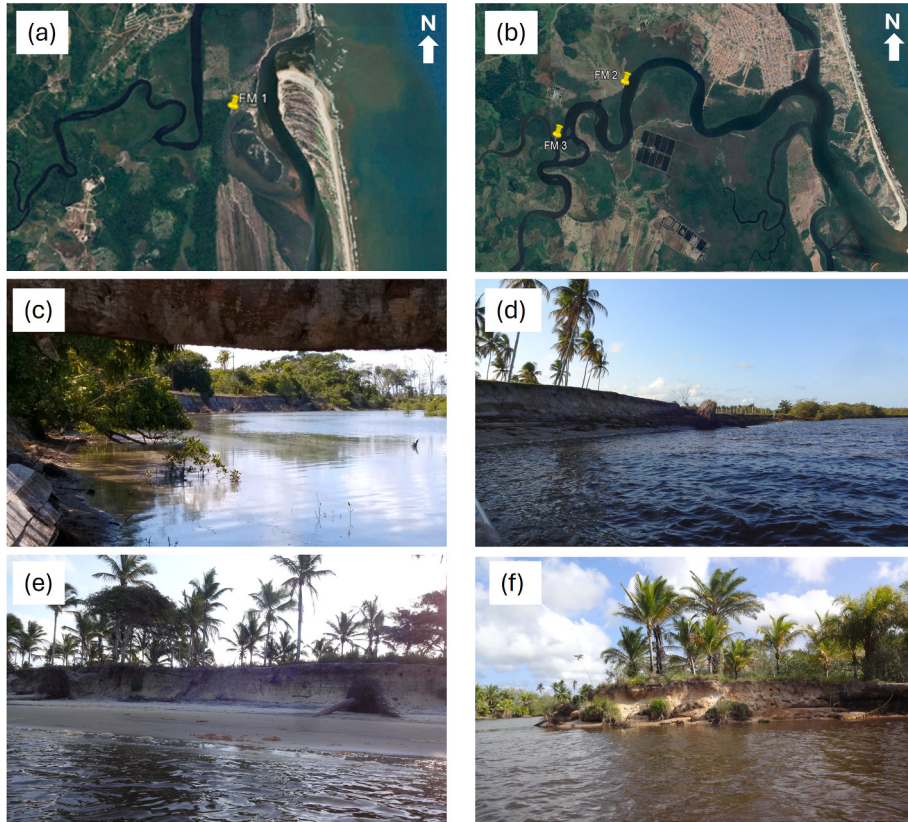


Fig. 2. – Aerial view and exposure of fluvimarine terrace along erosive riverbanks: (a) and (b) overview of sampling points FM1, FM2, and FM3; (c) NW-SE view of erosive slope at FM1; (d) SW-NE and (e) SE-NW views of erosive slope at FM2; (f) NW-SE view of erosive slope at FM3. Source: Google Earth, 2025; and field collection files.

vertical profiles and textural data visually, providing partially information regarding the erosional-depositional environment, hydrodynamics, pedogenesis, morphology, and variability in sediment supply (Folk and Ward, 1957; Miall, 1996; Empresa Brasileira de Pesquisa Agropecuária, 2018).

Therefore, the particle-size distribution was analyzed. From each identified layer, 20 g were fractionated and dried in an oven at 48 °C for 24 h. Then, the samples were mechanically fractionated from very coarse sand (2–1 mm/-1–0 φ) to clay (<0.002 mm/>9 φ). For the standard granulometric analysis in the sedimentological laboratory, we used an ASTM series of sieves with an interval ranging from 9 to –0.5 φ and a pipette for separating the silt and clay fractions, following the protocols of Camargo et al. (2009) and Empresa Brasileira de Pesquisa Agropecuária (2018).

To process and analyze each sample's grain-size and granulometric spindles, the SysGran v.4 was used (Camargo, 2006). This analysis included generating statistical parameters such as mean, median, sorting, skewness, kurtosis, cumulative curves, and textural classification (Folk and Ward, 1957). To determine the genetic-depositional environment of the analyzed samples, two granulometric diagrams proposed by Friedman (1967) and Martins (2003) were used. The diagrams were generated using Python version 3.9 as the programming language.

3.3. OSL geochronology

OSL geochronology was conducted on nine samples from three sites of fluviomarine terraces. Dark PVC tubes (6 cm in diameter and 60 cm in length) were used in each sampling and sent to the laboratory for preparation and luminescence dating of quartz grains, with granulometric fractions ranging from 100 to 250 µm (Cordier, 2010; Huntley et al., 1985; Murray and Wintle, 2000, 2003; Nelson et al., 2015). At each sampling site, the selection of the collection depth for OSL dating was based on stratigraphic discontinuities and contacts, aiming to date the middle age of different depositional events. Surface layers that were highly altered by bioturbation were excluded, as the incidence of solar radiation could potentially contaminate them.

The Single Aliquot Regeneration (SAR) protocol (Murray and Wintle, 2000, 2003; Wintle and Murray, 2006), using 15 or 25 aliquots with 3 mg of quartz grains, was used. Equivalent Doses (D_e) were determined using the SAR protocol, in which a dose-response curve was obtained for each aliquot. Additionally, dose recovery tests were conducted to verify the performance of the SAR protocol for the studied samples (Murray and Wintle, 2000; Rhodes, 2011). The final ages were obtained using the Central Age Model (CAM) (Galbraith et al., 1999). Generally, the CAM is recommended for samples with low overdispersion values (<30 %) (Cunningham and Wallinga, 2012; Galbraith and Roberts, 2012).

The annual dose rates received by each sediment sample were calculated by determining the concentration of radionuclides (Thorium - Th, Uranium - U, and Potassium - K), using the γ-spectroscopy method. Measurements were conducted with a NaI (Tl) detector, model 802-2, model 727, from Canberra Industries Inc. The Dating Laboratory Ltda., located in São Paulo, Brazil, was responsible for procedures to obtain the depositional ages. Finally, the grouped data from the OSL dating are presented in Table 1, which shows the main parameters quantified by the laboratory to achieve the results, as well as the depth and coordinates of the sampled sites.

4. Results

4.1. Morphostratigraphic settings and OSL ages

The stratigraphic columns were analyzed according to their morphosedimentary and morphopedological structures and modal grain-size, composing a hierarchy of processes in different coastal plain sectors. During their interpretations, the spatialization of the collection points was considered, since the marine and fluvial processes did not

Table 1
OSL ages obtained in the sampling sites.

Sample	Coordinates	Elevation a.s.l. (m)	Depth (cm)	Aliquot	Water (%)	Th (ppm)	U (ppm)	K (%)	Dose rate (µGy/ year)	Over-dispersion (%)	Cosmic dose rate (Gy/year)	De (Gy)	Age (ka)
FM1	15°17'41.59"S	3	80	15	4.5	2.447 ± 0.216	1.010 ± 0.119	1.693 ± 0.111	2.140 ± 95	7	170	3.1	1.46 ± 0.14
	39° 08'08"W		180	15	3.9	3.527 ± 0.246	1.337 ± 0.123	0.981 ± 0.098	1.620 ± 85	4	143	3.1	1.93 ± 0.20
FM1	15°17'41.59"S	3	310	15	3.7	2.838 ± 0.227	1.110 ± 0.120	0.776 ± 0.096	1.300 ± 80	1.5	115	3.5	2.66 ± 0.30
	39° 08'08"W		110	25	2.4	5.36 ± 0.27	0.978 ± 0.124	0.29 ± 0.1	1.040 ± 100	3	170	4.8	4.57 ± 0.48
FM2	15°41'0.42"S	6	160	25	0	1.63 ± 0.22	0.517 ± 0.113	0.45 ± 0.09	850 ± 100	≥ 0	160	4.5	5.30 ± 0.66
	38°58'35.41"W		20	25	28.3	11.01 ± 0.32	1.355 ± 0.124	0.23 ± 0.09	1.150 ± 80	≥ 0	180	12.1	10.59 ± 0.85
FM2	15°41'0.42"S	6	50	15	5.7	4.423 ± 0.273	0.839 ± 0.114	1.262 ± 0.101	1.840 ± 85	28	180	2.9	1.55 ± 0.18
	38°58'35.41"W		110	15	2.5	2.966 ± 0.232	0.839 ± 0.115	1.272 ± 0.105	1.760 ± 90	12	161	5.0	2.82 ± 0.32
FM3	15°41'33.88"S	4	170	15	7.9	1.928 ± 0.190	0.972 ± 0.108	0.861 ± 0.090	1.280 ± 75	9	145	4.4	3.44 ± 0.31
	38°59'23.98"W												
FM3	15°41'33.88"S	4											
	38°59'23.98"W												

advance and retreat in a linear fashion throughout the analyzed plain. Therefore, their OSL ages were expected to be divergent, but the morphostratigraphic and granulometric characteristics demonstrate similarities between the different correlated layers (Fig. 3).

In column FM1, a pronounced development of the pedogenetic layer is observed. In the first 50 cm of depth, horizon (A) presents a dark coloration and a strong influence of bioturbation, either by the action of roots or microfauna. This dark color is likely associated with the large amount of organic matter contributed by the forest vegetation that covers the analyzed fluviomarine terrace, and it is possible to observe the formation of leaf litter on the terrain's surface. The second horizon from 50 to 140 cm of depth begins with an abrupt transition, composed of a whitish albic eluvial layer (E), followed by a new abrupt horizon transition, characterized by the concentration of colloidal humic materials and clay (B) brown spodic at 190 cm of depth (Fig. 3). These characteristics are consistent with classic Spodosol profiles developed on sediments of marine and fluviomarine origin (Moreira et al., 2022).

At a depth of 190 cm, a gradual transition occurs, suggesting the advancement of pedogenesis over the parent material (marine sediments), which still exhibit well-defined plane-parallel stratification but already contain patches of mineral translocation in the profile. Furthermore, marine ichnofossils were observed in the transition between the two lower layers between 190 and 260 cm and 206–345 cm (Figs. 3 and 4) which, according to their apparent morphology, are *Ophiomorpha nodosa*, a species reported in several worldwide Pleistocene sedimentary deposits (Cheel and Leckie, 1993) and also on the Brazilian coast according to many authors (Tomazelli and Dillenburg, 2007; Lopes et al., 2014; Martins et al., 2018), but little reported in Holocene deposits in the Brazilian literature.

In column FM1, the central portion of the three depositional layers was dated by OSL. The most superficial layer, 80 cm, obtained a depositional age of 1.46 ± 0.14 ka, while at 180 cm, it was found to be 1.93 ± 0.20 ka, and at 310 cm, 2.66 ± 0.30 ka. According to Folk and Ward (1957), the modal fraction of the profile was all classified as fine sand.

The FM2 stratigraphic column also exhibits some pedogenetic development, but with a smaller apparent quantity of organic matter due to the pasture vegetation cover of the terrain. The superficial horizon (A) is 0–70 cm deep, after this layer the whitish albic eluvial horizon (E) is observed between 70 and 150 cm deep, followed by a new abrupt transition, which is characterized by the occurrence of a brown spodic horizon (B), but with a significantly reduced thickness of ~20 cm. Below lies a transitional layer, also not very thick, with a cream color, characterized as horizon (C) at the weathering front, without apparent stratification.

At a depth of 195 cm, an abrupt transition occurs in the FM2 stratigraphic column, modifying the modal pattern of sedimentation and changing from fine to very fine sand. In this layer, levels of sand are observed intercalated with bluish-colored silt/clay, indicating distinct hydrodynamic depositional conditions, probably from an estuarine environment. Regarding the ages obtained by OSL dating according to the previously established criteria, they result at 110 cm of depth as 4.57 ± 0.48 ka, at 160 cm depth as 5.30 ± 0.66 ka, and at 200 cm depth as 10.59 ± 0.85 ka, respectively, demarcating distinct phases in the early and middle Holocene.

The FM3 stratigraphic column exhibits lesser pedogenetic development compared to the other two profiles. It is the exposed column, presenting less depth and thickness of layers. The first dark brown layer is 30 cm deep, and strong bioturbation promoted by microfauna and

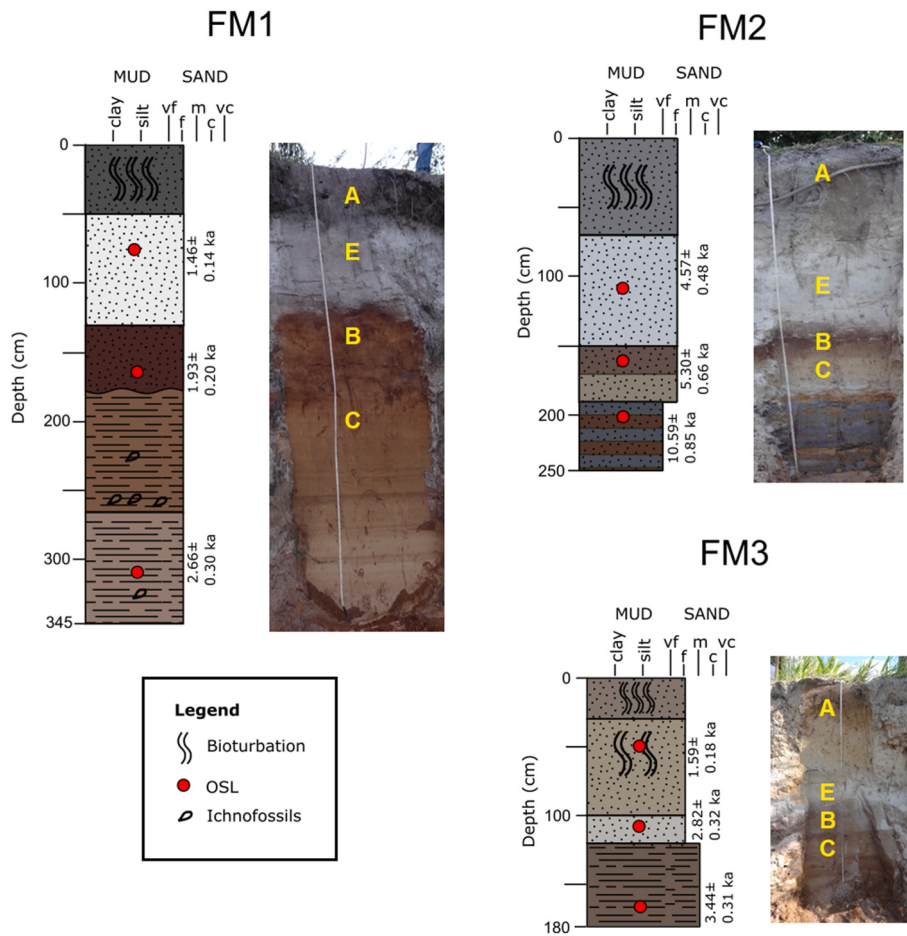


Fig. 3. Stratigraphic columns FM1, FM2 and FM3 with their respective morphological characteristics and OSL ages.



Fig. 4. – Cylindrical features of marine ichnofossils *Ophiomorpha nodosa* found in a horizontal position, aligned and dispersed in the profile from a depth of ~220 cm.

coconut tree roots, which are the predominant land use on this terrace, can be observed. Below, between 30 and 100 cm, a cream-colored layer is present that still exhibits bioturbation, primarily caused by the roots of the coconut trees, which is characterized as horizon (A).

Immediately below, a shallow albic horizon (E) is observed, 10 cm thick, as well as an equally shallow incipient spodic horizon (B) that is in contact with a layer in the weathering front that still maintains stratigraphic depositional characteristics that are parallel to the plane and continue to a depth of 180 cm. The modal fraction between depths 0 cm and 110 cm was identified as fine sand. Still, after this depth, there is an increase in the modal fraction to medium sand, which may characterize different depositional conditions. The OSL ages obtained for these layers are, at 50 cm, 1.59 ± 0.18 ka; 110 cm, 2.82 ± 0.32 ka; and 170 cm, 3.44 ± 0.31 ka, respectively.

4.2. Sedimentological analysis and morpho-depositional environments

The granulometric characteristics of soil and sediment samples provide significant information about erosional and depositional environments (Table 2) and (Fig. 5). The samples which have a higher cumulative mass retained at lower values of φ indicate that there are most coarser particles, while the samples with a higher percentage of mass retained at higher phi values, show a predominance of finer particles. The intermediate retained mass and φ values show a mixture of finer, medium and coarser sediments.

The analysis (Fig. 5d) revealed a relatively uniform distribution among the samples, primarily fine sediments. However, slight variations were observed in FM2 at 220 cm and FM3 at 50 cm, where the distribution shifted towards coarser particle diameters.

Two granulometric diagrams Friedman (1967) and the Martins (2003) diagram Fig. 6, were used to determine the genetic-depositional environment of the samples analyzed. The Friedman diagram (Fig. 6a) is based on the relationship between Sorting (σ_φ) and Skewness (Sk_φ) and

is employed to distinguish sediments of fluvial, dune, and coastal origin.

The Martins diagram (Fig. 6b) combines Mean (Mz_φ) and Sorting (σ_φ) to characterize different sedimentary environments. The separation curves in the diagram identify transitions between different environments: beach (B), dune (D), and river (R). The data used to construct these diagrams were derived from granulometric analysis of the samples. The extracted parameters, including mean grain size, sorting, and skewness, were expressed in phi units and used to plot the samples.

In the Friedman diagram (Fig. 6a), most samples are positioned between B and D, indicating a predominance of coastal-dune environments with some fluvial influences. Specifically, FM1 - 20 cm, FM1 - 80 cm, FM1 - 180 cm, FM1 - 260 cm, and FM1 - 310 cm cluster in the region of diagram area, associated with beach and dune environments, showing positive skewness and moderate sorting, which is typical of wind-transported and wave-influenced sediments. These features suggest a depositional setting where eolian and coastal processes play a dominant role in sediment selection.

Conversely, FM2 - 100 cm, FM2 - 170 cm, FM3 - 110 cm, and FM3 - 170 cm exhibit negative skewness and slightly poorer sorting, indicating a more significant influence of fluvial processes or sediment reworking. FM2 - 170 cm, which exhibits the most negative skewness value, suggests deposition in a transitional environment where different grain sizes are mixed due to the combined action of fluvial and tidal processes.

The Martins diagram (Fig. 6b) further supports these interpretations. Most of the samples, including FM1 - 20 cm, FM1 - 80 cm, FM1 - 180 cm, FM1 - 260 cm, FM1 - 310 cm, and FM2 - 100 cm are set in D, confirming their coastal-dune depositional setting. However, FM2 - 170 cm, which is positioned beyond B, indicates fluvial and/or interdune transitional processes, reinforcing the idea of sediment reworking and deposition in a more variable energy setting.

Distinct cases are FM3 - 50 cm and FM2 - 220 cm, which are characterized by very poor sorting and a broader grain size distribution, positioning them in a high-energy environment or a zone of strong

Table 2

Statistical data related to the 11 sediment samples analyzed. (M_z , grain mean size; σ , sorting; Sk_φ , skewness; k_G , kurtosis; M, median).

Sample	Sand	Silt	Clay	Classification (Folk and Ward, 1957)	M_z	σ	Sk_φ	k_G	M
	%				Φ				
FM1 - 20 cm	97.6	1.3	1.1	Fine Sand	2.593	0.5098	0.5313	0.6101	2.378
FM1 - 80 cm	98.8	0.1	1.1	Fine Sand	2.595	0.5051	0.5215	0.6015	2.385
FM1 - 180 cm	98	0.1	1.9	Fine Sand	2.484	0.46	0.5752	1.793	2.298
FM1 - 260 cm	98.5	0.5	1	Fine Sand	2.659	0.5168	0.3996	0.5765	2.486
FM1 - 310 cm	98.8	1.1	0.1	Fine Sand	2.614	0.5189	0.4629	0.5856	2.418
FM2 - 100 cm	98.3	0.7	1	Fine Sand	2.27	0.4204	0.03414	2.624	2.27
FM2 - 170 cm	98.4	0.1	1.5	Fine Sand	2.064	0.5841	-0.2539	2.546	2.237
FM2 - 220 cm	66.5	18.2	15.3	Very Fine Sand	3.844	1.926	0.5345	0.9078	3.295
FM3 - 50 cm	91.7	1.8	6.5	Fine Sand	2.563	1.346	0.6504	3.093	2.326
FM3 - 110 cm	98.3	0.2	1.5	Fine Sand	2.018	0.6157	-0.2735	2.49	2.216
FM3 - 170 cm	98	0.6	1.4	Medium Sand	1.998	0.6195	-0.2962	2.552	2.204

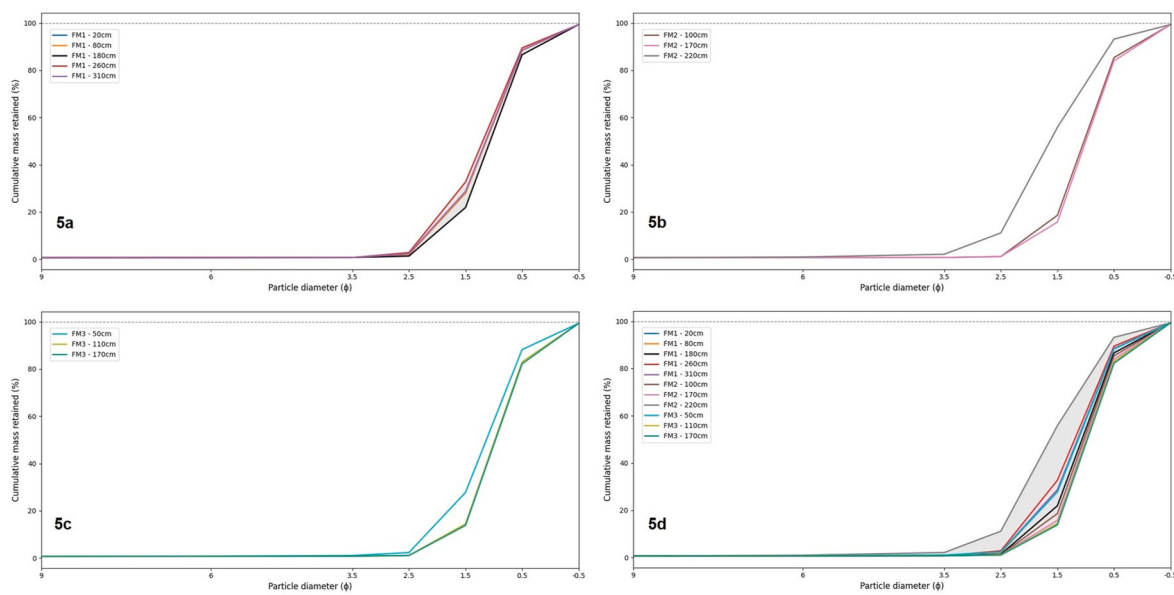


Fig. 5. Graphs of the cumulative frequency curves of the collected samples. **Fig. 5a:** Represents FM1 samples at the depths of 20, 80, 180, 260, and 310 cm. **Fig. 5b:** Represents FM2 samples at 100, 170, and 220 cm of depth. **Fig. 5c:** Represents FM3 samples at 50, 110, and 170 cm of depth. **Fig. 5d:** Granulometric spindle of the cumulative frequency curves for all collected samples. The legend is included above the graphs.

sediment reworking. Similarly, FM3 - 110 cm and FM3 - 170 cm also exhibit poor sorting and negative skewness, suggesting a more dynamic setting, possibly affected by intermittent fluvial input or reworking processes at the beach-dune interface.

The combined analysis of both diagrams highlights that coastal and dune environments predominantly influence the FM1 series samples, while the FM2 and FM3 ones display transitions towards fluvial or interdune deposits, with FM3 - 50 cm and FM2 - 220 cm standing out as the most poorly sorted sample (Fig. 6a), indicating a highly dynamic environment. These results suggest that sedimentation processes were influenced by both eolian transport and hydrodynamic action, with local variations in sorting and grain distribution due to differences in tractive capacity and sediment sources.

5. Discussion

The results highlighted that the different depositional events, identified in the three stratigraphic columns and cumulative frequency curves (Figs. 3 and 5), are characterized by distinct morphological and granulometric aspects, reinforcing the influence of a mixed environment in their formation — a determining characteristic in this transitional environment. Therefore, correlation with other studies and environmental contexts is necessary to gain a better understanding of the Holocene and paleoclimatic dynamics of the fluviomarine terraces.

5.1. Environmental depositional conditions and pedogenesis process

It is worth noting that after the consolidation of the analyzed sediments, current and past pedogenesis, as well as bioturbation, altered some of the depositional characteristics, leading to new interpretations regarding the vertical distribution of particles and organic material. According to Rossi et al. (2021), the pedogenetic development of Spodosols in coastal environments strongly correlates with fluctuations in the water table, vegetation, and depressions between coastal ridges. In this sense, oscillations in climatic conditions during the Holocene may have influenced water availability and, consequently, soil drainage, thereby affecting the advancement or stagnation of pedogenetic processes (Moreira et al., 2022).

This relationship is widely discussed by Lopes-Mazzetto et al. (2018)

and Martinez et al. (2018), who analyzed transects of Spodosols on the southeastern coast of Brazil, obtaining absolute ages of 5.2 ± 0.8 and 3.6 ± 0.3 ka for marine terraces where the soils formed under limited drainage circumstances, that is, in environmental and climatic conditions different from the current ones. Additionally, according to these authors, the drainage conditions observed in the terraces dated between 3.2 ± 0.3 , 1.4 ± 0.1 , and 1.1 ± 0.9 ka were more intense and vertical. Thus, it was concluded that younger Spodosols and those close to the current coastline are not undergoing degradation, as they were formed under more recent drainage conditions, indicating that they still undergo active translocation processes.

Lopes-Mazzetto et al. (2018) concluded that while the transitions between the (E) and (B) horizons in poorly drained podzols are generally flat and horizontal, the top of the (B) horizon may lose organic matter after improved drainage in wetter periods. Thus, the (E-B) boundary may become gradual so that the (E-B) and (B-E) horizons can be distinguished. Thus, the increase in drainage due to the new environmental conditions may cause the dominance of vertical movement over lateral water dynamics.

These conclusions are similar to the environmental conditions observed in the fluviomarine terraces of this research, where the FM1 profile, located closer to the current coastline, exhibits more recent ages and apparent vertical translocation between horizons (E, B, C). In contrast, the FM2 and FM3 profiles presented older ages and had abrupt contacts between the same horizons, indicating that post-formations had predominantly horizontal drainage.

Regarding the results of the morpho-depositional analyses presented mainly in the diagrams of Friedman (1967) and Martins (2003), they indicated a significant influence of wind remobilization in the FM2 and FM3 deposits, such characteristics were not corroborated by the stratigraphic columns or by previous works in the region (Bacoccoli, 1971; Martin et al., 1980; Dominguez et al., 2023; Martin et al., 1993). The lack of dune fields currently in the study area is also an indication that the winds in the region are not capable of transporting large quantities of particles, in addition to the water table conditions, which remain very superficial throughout the year, making wind transport impossible and fixing vegetation on the fluviomarine terraces, as well as in the mangroves.

Therefore, the wind remobilization indicated in the graphs suggests

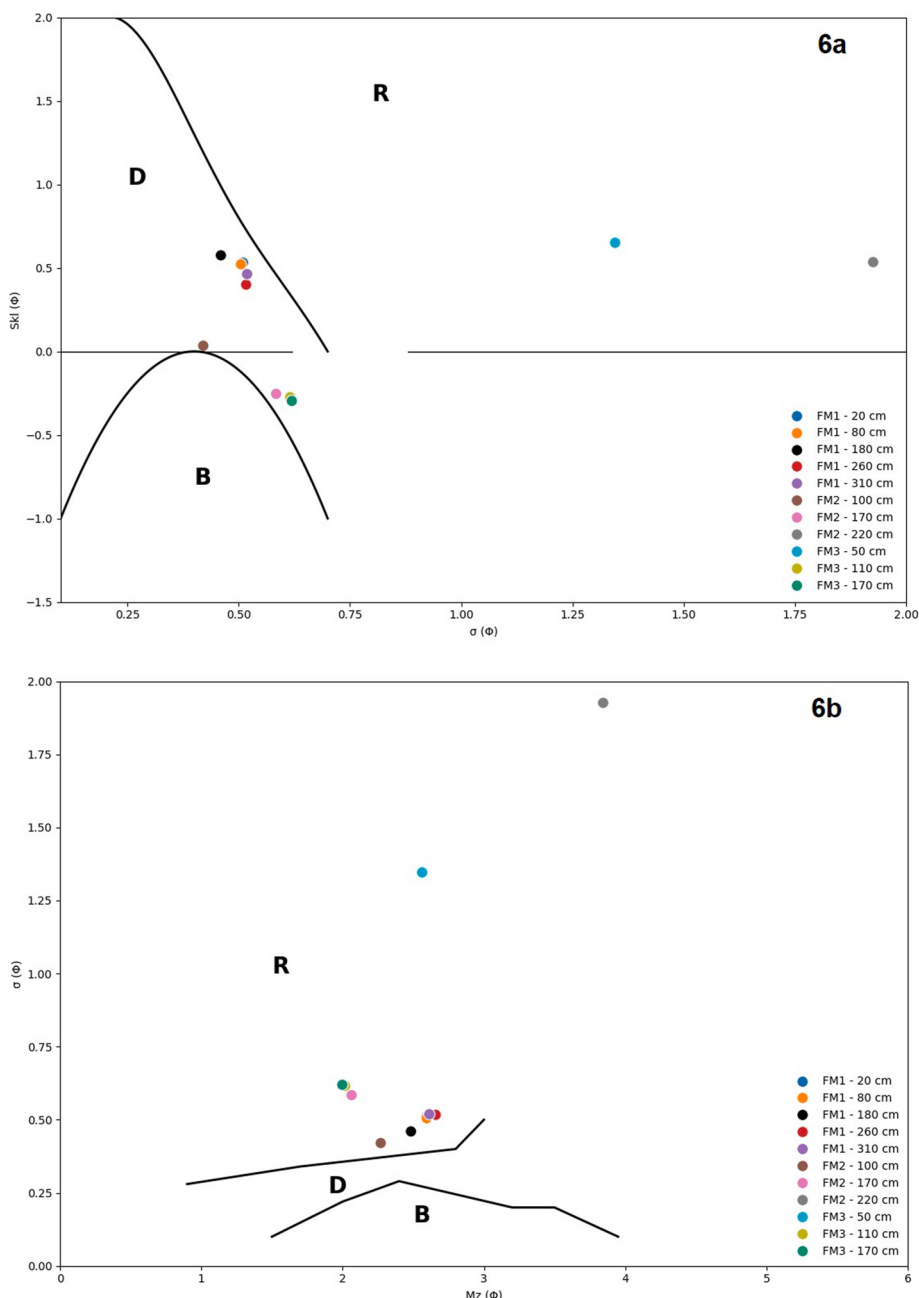


Fig. 6. a: Friedman (1967) diagram based on the relationship between $\sigma(\Phi)$ and $Sk(\Phi)$ for the classification of the environment of the same area. B - Beach environment, D - Dune environment, R - Fluvial environment. The legend is included below the graphs; b: Martins (2003) diagram is based on the relationship between $Mz(\Phi)$ and $\sigma(\Phi)$ for the classification of the genetic-depositional environment of samples from fluviomarine terraces. In both diagrams: B is Beach, D is Dune, and R is the River environment.

that it is a specific, short-term, local phenomenon that does not correspond to the regional environmental characteristics. This fact can be confirmed by Correia Filho and Aragão (2014), who analyzed the temporal wind patterns in mesoregions of the state of Bahia, demonstrating the importance of local factors in this dynamic. According to Moreira et al. (2024), morphologically, the marine deposits in the region appear as sequences of beach ridges on a regressive trend, that is, they are only slightly reworked after consolidation.

5.2. Holocene climatic events and influence on fluviomarine terraces

When observing the distribution of ages obtained in different depositional layers of fluviomarine terraces, the grouping of data in specific

phases during the Holocene becomes evident. This suggests a possible correlation with climatic events that affected the region, resulting in variations in river discharge and RSL. Such depositional dating groupings will be correlated with the depositional ages of beach ridges dated by Moreira et al. (2024) close to the investigated terraces and sea level curves constructed for the last 11 ka for the Brazilian coast.

We will begin the discussion with the set of the oldest deposits found on the fluviomarine terrace at FM2, which at a depth of 220 cm had a depositional age of 10.59 ± 0.85 ka and the morpho-sedimentary aspects indicate a high-energy environment or an area of strong sediment reprocessing. In this period (Late Holocene), the sea level was lower than it is today in the Brazilian Northeast coast (Suguió et al., 1985; Alves and Rossetti, 2017), and according to Moreira et al. (2024), the inland

estuarine systems were formed near the outlet of the Pardo River during this period, which explains the clay laminations interspersed with sand in this layer. This is a climatic period immediately after the Younger Dryas, as described by Rasmussen et al. (2014), and therefore brought more rainfall to the tropics (Strfkis et al., 2011; Mescolotti et al., 2021; Chiessi, 2021), which may have influenced the more significant contribution of sediment and river water to the estuary (Fig. 7). Notably, in the lower Holocene, ~8 ka, the RSL was ~4 m below the current level (Suguió et al., 1985; Martin et al., 2003; Angulo et al., 2006; Alves and Rossetti, 2017). This context effectively characterizes the environmental conditions of the Early Holocene for the coastal plain of the Pardo River.

Subsequently, Fontes et al. (2017), Cohen et al. (2005), Lorente et al. (2020), and Martins et al. (2021) describe deposits in estuarine systems that advanced upstream between ~7.4 and 5.3 ka and are currently up to 34 km upstream of the current coastline. Climatic conditions of lower humidity may have generated the peak of the marine influences' advance.

The two most superficial layers of the FM2 terrace yielded mid-Holocene ages of 4.57 ± 0.48 ka at a depth of 110 cm and 5.30 ± 0.66 ka at a depth of 160 cm. These two layers, although morphologically distinct due to the action of soil formation, will be interpreted together. These deposits were consolidated during and shortly after the Holocene transgressive maximum, between ~6 and 5 ka (Suguió et al., 1985; Martin et al., 2003; Angulo et al., 2006; Alves and Rossetti, 2017; Tomazelli and Dillenburg, 2007; Dominguez et al., 2021, 2023), when sea level was ~3–4 m higher than it is today. According to sedimentological analysis, these deposits are characterized as marine/eolian and transitional. Corroborating this information, Martin et al. (1993) and Moreira et al. (2024) identified the formation of barrier islands and marine terraces during this period in the Jequitinhonha delta region (Fig. 1).

Advancing the discussion, we will correlate the deposit of point FM3 at 170 cm depth, which obtained a dating of 3.44 ± 0.31 ka with regional events. According to sedimentological analysis, these are fluvial deposits, which in our interpretation may be associated with the response of the last rise in RSL. Dominguez (1982) and Moreira et al. (2024), describe that last rise in the RSL influenced the migration of the outlets of the Jequitinhonha and Pardo rivers. The authors suggest that the Jequitinhonha River migrated in search of a position that would allow for better adjustment and energetic efficiency, influenced by the last regional rise of the RSL that occurred during the same period. Furthermore, it is noteworthy that the wetter phases of the Middle and Late Holocene are mainly associated with the Bond events (Fig. 7), which in turn are linked to the southward displacement of the Intertropical Convergence Zone - ITCZ, during periods of cooling in the North Atlantic Novello et al. (2018). They have been identified as climatic pulses by Perez Filho et al. (2022).

The deposits dated ~2.5 ka (FM3 2.82 ± 0.32 at 110 cm and FM1 2.66 ± 0.30 at 310 cm depth, characterized with fluvial and marine/aeolian origin respectively) are correlated with the consolidation of the second generation of the second level of marine terraces, according to Moreira et al. (2024). During this period, the current outlets of the Jequitinhonha and Pardo rivers were established, following the continuous rhythm of coastal progradation and the formation of channels in a north-south direction parallel to the coast, due to the creation of new barrier islands at the front. Additionally, extensive areas of mangroves were formed in the transition environment.

From this perspective, rainfall correlated with the strengthening of the South Atlantic Convergence Zone - SACZ observed in the Late Holocene could supply the drainage headwaters of the Brazilian Atlantic Plateau, increasing the volume, flow, transported sediment load and flood pulses of rivers that flow into the Atlantic Ocean (Rodrigues et al., 2016), thus contributing to the deposition of sediments of fluvial origin on the fluviomarine terraces (Perez Filho et al., 2022).

Finally, the deposits with more recent ages and, therefore, are more superficial (FM3 1.59 ± 0.18 ka at 50 cm and FM1 1.46 ± 0.14 ka and

1.93 ± 0.20 ka at 80 cm and 180 cm depth) are associated with the Bond 1 event (Bond et al., 1997; Strfkis et al., 2011). This phenomenon correlates with the establishment of the current cusp shape of the Jequitinhonha Delta and the formation of the marine terrace level one, characterized by the increase and establishment of the current frontal barrier islands (Moreira et al., 2024). From this, it is recognized that the sampled interior fluviomarine terraces, FM2 and FM3, had contributions of sediments of fluvial and/or aeolian origin, as they were already far from the coastline at that time. However, FM1 may have been affected by marine sedimentation due to its proximity to the current coastline.

Fig. 7 presents a summary of the climatic events associated with the deposits characterized and dated in this study, as well as the three levels of marine terraces dated by Moreira et al. (2024), which contribute to the local paleoenvironmental interpretation.

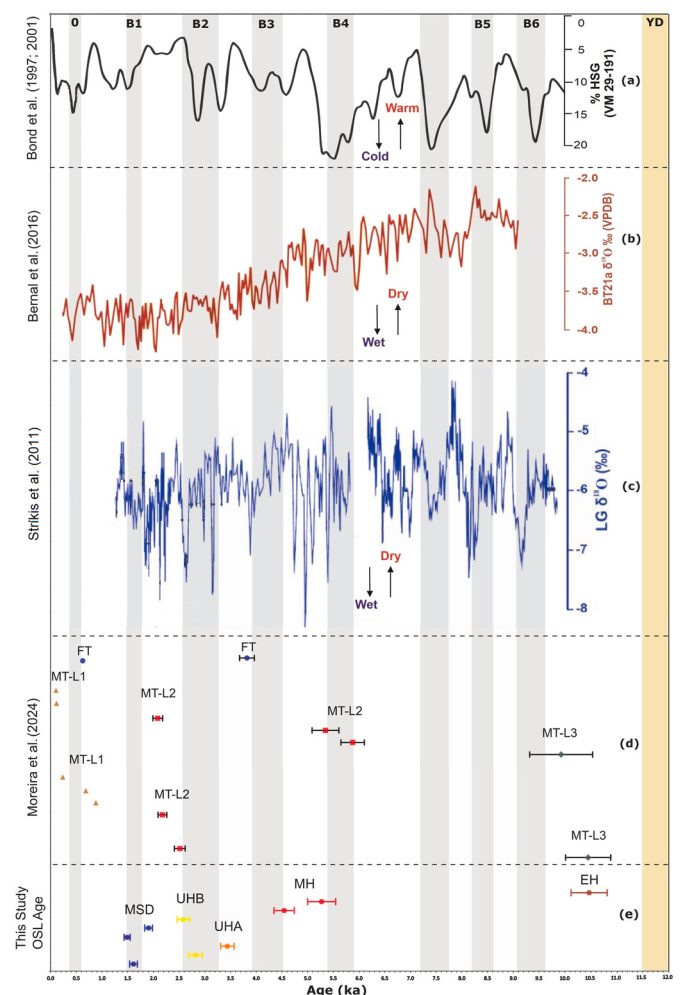


Fig. 7. Synthesis of the five depositional stages in the fluviomarine terraces, associated Holocene climatic events, and stages defined for the study area. (a) Record of hematite-stained quartz grains (HSG) from the North Atlantic marine core VM 29-191 (Bond et al., 1997, 2001). (b) Composite record of $\delta^{18}\text{O}$ from stalagmite BT21a, Botuverá cave, Southern Brazil (Bernal et al., 2006). (c) Composite record of $\delta^{18}\text{O}$ from stalagmites LG3 and LG11, Lapa Grande cave, central-eastern of Brazil. (d) OSL datings by (Moreira et al., 2024) where FT: Fluvial terrace; MT-L1: Marine Terrace Level 1; MT-L2: Marine Terrace Level 2; MT-L3: Marine Terrace Level 3. (e) Stages defined according to the grouping of ages of depositional events of fluviomarine terraces where MSD: Modern Surface Deposits; UHB: Late Holocene B; UBA: Late Holocene A; MH: Medium Holocene; EH: Early Holocene. The gray columns represent successive Bond events. The brown column represents the Young Dryas event. Source: Perez Filho et al. (2022). Adapted by the authors.

6. Conclusions

The analyzed fluviomarine terraces served as an excellent indicator of environmental changes during the Holocene, as their genesis is closely linked to the climatic pulses that altered the sedimentary balance of the Pardo River estuary. These results corroborate the large-scale studies on the morphodynamics of the Brazilian coast and elucidate local aspects of geomorphological and paleogeographic development of this estuary based on the differentiation of five main distinct stages:

1. (Early Holocene $\sim 10.59 \pm 0.85$ ka) With the RSL ~ 4 m below the current level, an inland estuarine system near the Pardo River mouth predominated in the study area, which was also influenced by a drier climate, where a continuous succession of fine and coarse deposits was observed at times of greater or lesser fluvial influence;
2. (Middle Holocene $\sim 5.30 \pm 0.66$ and 4.57 ± 0.48 ka) After the Holocene transgressive maximum reported along the entire Brazilian coast, where the RSL was from ~ 3 to 4 m higher than the current one in the study area, the formation of marine and aeolian deposits predominated over the ancient estuary, enabling the formation of spodic profiles in a drier climate than the current one;
3. (Late Holocene A $\sim 3.44 \pm 0.31$ ka) The last elevation of the local RSL occurred, which promoted migration of the outlets of the Pardo and Jequitinhonha rivers and stabilization of pedogenetic processes in ancient spodic profiles. Bond climate events and the displacement of the ITCZ may be associated with this environmental change;
4. (Late Holocene B ~ 2.5 ka) With the strengthening of the SACZ, the formation of a new generation of marine terraces and barrier islands occurs, due to the greater sedimentary input of the rivers in the Jequitinhonha River estuary and delta;
5. (Modern Surface Deposits $\sim 1.93 \pm 0.20$; 1.59 ± 0.18 and 1.46 ± 0.14 ka) In this last phase, new sedimentation occurred on the fluviomarine terraces due to a significant river supply, associated with the Bond 1 event. In these deposits, vertical translocations are observed in younger Spodosol profiles, demonstrating the reactivation of vertical translocation, which differentiates them from the older deposits.

CRediT authorship contribution statement

Vinicius Borges Moreira: Writing – review & editing, Writing – original draft, Visualization, Validation, Software, Methodology, Investigation, Formal analysis, Data curation, Conceptualization. **Luca Lämmle:** Writing – review & editing, Methodology, Investigation, Formal analysis, Data curation, Conceptualization. **Mariarca D'Aniello:** Writing – review & editing, Software, Methodology, Investigation, Data curation. **Fabiano Tomazini Da Conceição:** Writing – review & editing, Supervision, Methodology, Formal analysis, Conceptualization. **Carlo Donadio:** Writing – review & editing, Methodology, Formal analysis, Conceptualization. **Archimedes Perez Filho:** Writing – review & editing, Supervision, Project administration, Methodology, Funding acquisition.

Declaration of competing interest

The authors declare that they have no known competing financial interests or personal relationships that could have appeared to influence the work reported in this paper.

Acknowledgements

The authors are grateful to the São Paulo Research Foundation (FAPESP) for the support through process n° 2016/21335-9, 2023/16236-5, and 2023/05346-4.

Data availability

The data presented in this study are available upon request from the corresponding author or any other authors of this research.

References

- Ab'Sáber, A.N., 1955. Contribuição a geomorfologia do litoral paulista. *Rev. Bras. Geogr.* 17 (1), 3–48. Rio de Janeiro.
- Aiello, G., Barra, D., Collina, C., Piperno, M., Guidi, A., Stanislao, C., Saracino, M., Donadio, C., 2018. Geomorphological and paleoenvironmental evolution in the prehistoric framework of the coastland of Mondragone, southern Italy. *Quat. Int.* 493, 70–85. <https://doi.org/10.1016/j.quaint.2018.06.041>.
- Alves, F.C., Rossetti, D.F., 2017. Late Holocene coastal dynamics and relative sea-level changes in the littoral of Paraíba, northeastern Brazil. *Prog. Phys. Geogr. Earth Environ.* 41 (4), 375–392. <https://doi.org/10.1177/030913317709744>.
- Angulo, R.J., Lessa, G.C., Souza, M.C., 2006. A critical review of mid- to late-Holocene sea-level fluctuations on the eastern Brazilian coastline. *Quat. Sci. Rev.* 25 (5–6), 486–506. <https://doi.org/10.1016/j.quascirev.2005.03.008>.
- Araújo, V.D., Reyes-Perez, Y.A., Lima, R.O., Pelosi, A.P.M.R., Menezes, L., Córdoba, V.C., Lima-Filho, F.P., 2006. Fácies e sistema deposicional da formação barreiras na região da Barreira do Inferno, litoral oriental do Rio Grande do Norte. *Geologia USP. Série Científica* 6 (2), 43–49. <https://doi.org/10.5327/s1519-874x2006000300006>.
- Arnaud-Fassetta, G., 2003. River channel changes in the Rhone Delta (France) since the end of the little ice age: geomorphological adjustment to hydroclimatic change and natural resource management. *Catena* 51 (2), 141–172. [https://doi.org/10.1016/S0341-8162\(02\)00000](https://doi.org/10.1016/S0341-8162(02)00000).
- Arruda, D.L., Ker, J.C., Schaefer, C.E., Melo, H.F., Camélo, D.L., Paes, E.C.P., Barroso, S.H., 2023. Unraveling the sedimentation environment of Marajó Island: insights from geochemical studies and implications for the origin of potentially toxic element in soils. *J. S. Am. Earth Sci.* 128, 104452. <https://doi.org/10.1016/j.jsames.2023.104452>.
- Bacoccoli, G., 1971. Os deltas marinhos holocênicos brasileiros: uma tentativa de classificação. *Bol. Tec. Petrobras* 14 (1–2), 5–38.
- Barra, B., Donadio, C., Lämmle, L., Perez Filho, A., Stamatopoulos, L., Valente, A., Kontopoulos, N., Parisi, R., Stanislao, C., Aiello, G., 2024. Morphogenetic and palaeoenvironmental evolution of the Lagoon of Kotychi in Western Peloponnese, Greece, during the Holocene. *Quat. Int.* 710, 66–94. <https://doi.org/10.1016/j.quaint.2024.07.014>.
- Bernal, J.P., Cruz, F.W., Strikis, N.M., Wang, X., Deininger, M.M., Catunda, M.C.A., Ortega-Obregón, C., Cheng, H., Edwards, R.L., Auler, A.S., 2006. High-resolution Holocene South American monsoon history recorded by a speleothem from Botuverá cave, Brazil. *Earth Planet Sci. Lett.* 245, 186–196. <https://doi.org/10.1016/j.epsl.2006.06.008>.
- Bond, G., Kromer, B., Beer, L., Muscheler, R., Evans, M.N., Showers, W., Hoffmann, S., Lotti-Bond, R., Hajdas, I., Bonani, G., 2001. Persistent solar influence on North Atlantic climate during the Holocene. *Science* 294, 2130–2136. <https://doi.org/10.1126/science.1065680>.
- Bond, G., Showers, W., Cheseby, M., Lotti, R., Almasi, P., Menocal, P., Priore, P., Cullen, H., Hajdas, I., Bonani, G., 1997. A pervasive millennial-scale cycle in the North Atlantic Holocene and glacial climates. *Science* 278, 1257–1266. <https://doi.org/10.1126/science.278.5341.1257>.
- Buso Junior, A.A., Pessenda, L.C.R., Oliveira, P.E., et al., 2013. From an estuary to a freshwater lake: a paleo-estuary evolution in the context of Holocene sea-level fluctuations, SE Brazil. *Radiocarbon* 55 (2–3), 1735–1745. <https://doi.org/10.1017/S003822200048657>.
- Camargo, M.G., 2006. Sysgran: um sistema de código aberto para análises granulométricas do sedimento. *Rev. Bras. Geociências* 36 (2), 371–378.
- Camargo, O.A., Moniz, A.C., Jorge, J.A., Valadares, J.M.A.S., 2009. Métodos de análise química, mineralógica e física de solos do Instituto Agronômico de Campinas, vol. 77. Campinas: Instituto Agronômico, 106.
- Cheel, R.J., Leckie, D.A., 1993. Hummocky cross stratification. In: Wright, V.P. (Ed.), *Sedimentology Review 1*. Blackwell Scientific Publications, Oxford, pp. 103–122.
- Chiessi, C.M., Mulitza, S., Taniguchi, N.K., Prange, M., Campos, M.C., Häggi, C., et al., 2021. Mid- to late-holocene contraction of the intertropical convergence zone over northeastern South America. *Paleoceanogr. Paleoclimatol.* 36 (4), 3936. <https://doi.org/10.1029/2020PA003936>.
- Cohen, M.C.L., Behling, H., Lara, R.J., 2005. Amazonian mangrove dynamics during the last millennium: the relative sea-level and the little ice age. *Rev. Palaeobot. Palynol.* 136 (1–2), 93–108. <https://doi.org/10.1016/j.revpalbo.2005.05.002>.
- Correia Filho, W., Aragão, M.J.R.S., 2014. Padrões temporais do vento à superfície em mesorregiões do Estado da Bahia. *Cienc. Nat.* 36 (2), 402–414. <https://doi.org/10.5902/2179460X13162>.
- Cordier, S., 2010. Optically stimulated luminescence dating: procedures and applications to geomorphological research in France. *Géomorphol. Relief, Process. Environ.* 16 (1), 21–40. <https://doi.org/10.4000/géomorphologie.7785>.
- CPRM - Companhia de Pesquisa de Recursos Minerais, 2006. Geobank – geologia - folha itapetinga (SD.24-Y-D). Disponível em: <http://geosgb.cprm.gov.br/>.
- CPRM - Companhia de Pesquisa de Recursos Minerais, 2010. Geobank – geomorfologia – mapa de Geodiversidade do Estado da Bahia. Disponível em: <http://geosgb.cprm.gov.br/>.
- Cunningham, A.C., Wallinga, J., 2012. Realizing the potential of fluvial archives using robust OSL chronologies. *Quat. Geochronol.* 12, 98–106. <https://doi.org/10.1016/j.quageo.2012.05.007>.

- De Miranda, L.B., Andutta, F.P., Kjerfve, B., Castro Filho, B.M., 2017. Fundamentals of Estuarine Physical Oceanography. Springer, Singapore, p. 480. <https://doi.org/10.1007/978-981-10-3041-3>.
- De Pippo, T., Donadio, C., Pennetta, M., 2001. Morphological evolution of Lèsina Lagoon (Southern Adriatic, Italy). *Geogr. Fis. Din. Quaternaria* 24 (1), 29–41.
- De Pippo, T., Donadio, C., Pennetta, M., 2000. Evoluzione morfologica della Laguna di Sabaudia (Mar Tirreno, Italia centrale). *-2002 Geol. Rom.* 36, 1–12.
- Dillenburg, S.R., Barboza, E.G., Rosa, M.L.C.C., Caron, F., Sawakuchi, A.O., 2017. The complex prograded Cassino barrier in southern Brazil: geological and morphological evolution and records of climatic, oceanographic and sea-level changes in the last 7–6ka. *Mar. Geol.* 390, 106–119. <https://doi.org/10.1016/j.margeo.2017.06.007>.
- Dominguez, J.M.L., Kikuchi, R.K.P., Araújo Filho, M.C., Schwamborn, R., Vital, H., 2023a. The wave-dominated deltas of Brazil. (Org.) Tropical Marine Environments of Brazil: Spatio-Temporal Heterogeneities and Responses to Climate Changes. the Latin American Studies Book Series, first ed. Springer International Publishing, Switzerland.
- Dominguez, J.M.L., Guimarães, J.K., 2021. Effects of holocene climate changes and anthropogenic river regulation in the development of a wave-dominated delta: the São Francisco river (Eastern Brazil) *Mar. Geol.* 435, 106456. <https://doi.org/10.1016/j.margeo.2021.106456>.
- Dominguez, J.M.L., 1982. Evolução quaternária da planície Costeira associada à foz do Rio Jequitinhonha (BA): Influência das variações do nível do mar e da deriva litorânea de sedimentos, vol. 73p. Salvador (Dissertação de Mestrado - Universidade Federal da Bahia). 73pp.
- Dominguez, J.M.L., Guimarães, J.K., Stattegger, K., Tanajura, E.L.X., 2023b. 3D depositional architecture of a wave-dominated delta in a far-field GIA region: the case of the São Francisco delta, Brazil. *Mar. Geol.* 464, 107145. <https://doi.org/10.1016/j.margeo.2023.107145>.
- Donadio, C., Stamatopoulos, L., Stanislao, C., Pennetta, M., 2018. Coastal dune development and morphological changes along the littorals of Garigliano, Italy, and Elis, Greece, during the Holocene. *J. Coast Conserv.* 22 (5), 847–863. <https://doi.org/10.1007/s11852-017-0543-3>.
- Empresa Brasileira de Pesquisa Agropecuária (EMBRAPA), 2018. Sistema Brasileiro de Classificação de Solos, 5a ed. EMBRAPA, Brasília, p. 355. Revista e Ampliada.
- Folk, R.L., Ward, W., 1957. Brazos river bar: a study in the significance of grain size parameters. *J. Sediment. Res.* 27, 3–26. <https://doi.org/10.1306/74D70646-2B21-11D7-8648000102C1865D>.
- Fontes, N.A., Moraes, C.A., Cohen, M.C.L., Alves, I.C.C., França, M.C., Pessenda, L.C.R., 2017. The impacts of the middle Holocene high sea-level stand and climatic changes on mangroves of the Jucuruçu river, southern Bahia – northeastern Brazil. *Radiocarbon* 59 (1), 215–230. <https://doi.org/10.1017/RDC.2017.6>.
- Friedman, G.M., 1967. Dynamic processes and statisticalparameters compared for size frequency distributionof beach and river sands. *J. Sediment. Petrol.* 37, 327–354.
- Galbraith, R.F., Roberts, R.G., 2012. Statistical aspects of equivalent dose and error calculation and display in OSL dating: an overview and some recommendations. *Quat. Geochronol.* 11, 1–27. <https://doi.org/10.1016/j.quageo.2012.04.020>.
- Galbraith, R.F., Roberts, R.G., Laslett, G.M., Yoshida, H., Olley, J.M., 1999. Optical dating of single and multiple grains of quartz from Jimmum rock shelter, northern Australia: part I. Experimental design and statistical models. *Archaeometry* 41, 339–364. <https://doi.org/10.1111/j.1475-4754.1999.tb00987.x>.
- Georgiou, N., Stocchi, P., Casella, E., Rovere, A., 2024. Decoding the interplay Between tidal notch geometry and sea-level variability during the last interglacial (Marine isotope stage 5e) high stand. *Geophys. Res. Lett.* 1 (6), e2023GL106829. <https://doi.org/10.1029/2023GL106829>.
- Godiva, D., Evangelista, H., Kampel, M., Licinio, M.V., Munita, C., 2010. Combined use of aerogammastrometry and geochemistry to access sediment sources in a shallow coral site at Armação dos Búzios, Brazil. *Estuarine, Coastal Shelf Sci.* 87 (4), 526–534. <https://doi.org/10.1016/j.ecss.2010.02.006>.
- Huntley, D.J., Godfrey-Smith, D.I., Thewalt, M.L.W., 1985. Optical dating of sediments. *Nature* 313, 105–107. <https://doi.org/10.1038/313105a0>.
- Köppen, W., 1936. Das geographische System der Klimate. In: Köppen, W., Geiger, R. (Eds.), *Handbuch der Klimatologie*, vol. I. Gebrüder Borntraeger, Berlin, p. 44. Part C.
- Kottek, M., Grieser, J., Beck, C., Rudolf, B., Rubel, F., 2006. World map of the Köppen-Geiger climate classification updated. *Meteorol. Z.* 15, 259–263. <https://doi.org/10.1127/0941-2948/2006/0130>, 263.
- Lämmle, L., Perez Filho, A., Donadio, C., Arienzo, M., Ferrara, L., Santos, C.J., Souza, A. O., 2022a. Anthropogenic pressure on hydrographic basin and coastal erosion in the Delta of Parába do Sul river, Southeast Brazil. *J. Mar. Sci. Eng.* 10 (11), 1585. <https://doi.org/10.3390/jmse10111585>.
- Lämmle, L., Perez Filho, A., Donadio, C., Moreira, V.B., Santos, C.J., Souza, A.O., 2022b. Baixos terraços marinhos associados às transgressões e regressões marinhas holocênicas na Planície Costeira do rio Parába do Sul, Rio de Janeiro, Brasil. *Revista Brasileira de Geomorfologia* 23, 1285–1303. <https://doi.org/10.20502/rbg.v23i2.1992>.
- Laprida, C., Chaporri, N.G.C., Violante, R.V., Compagnucci, R.H., 2007. Mid-holocene evolution and paleoenvironments of the shoreface–offshore transition, north-eastern Argentina: new evidence based on benthic microfauna. *Mar. Geol.* 240 (1–4), 43–56. <https://doi.org/10.1016/j.margeo.2007.02.001>.
- Lauff, G.H., 1967. *Estuaries*, vol. 83. Am. Assoc. Adv. Sci. Publ., Washington, D.C., p. 757p.
- Lopes, R.P., Dillenburg, S.R., Cesar, L., Schultz, C.L., et al., 2014. The sea-level highstand correlated to marine isotope stage (MIS) 7 in the coastal plain of the state of Rio Grande do Sul, Brazil. *Annals Braz. Acad. Sci.* 86 (4), 1573–1595. <https://doi.org/10.1590/0001-3765201420130274>.
- Lopes-Mazzetto, J.M., Buurman, P., Schellekens, J., Martinez, P.H.R.M., Vidal-Torrado, P., 2018. Soil morphology related to hydrology and degradation in tropical coastal podzols (SE Brazil). *Catena* 162, 1–13. <https://doi.org/10.1016/j.catena.2017.11.007>.
- Lorente, F.L., Castro, D.F., Francisquini, M.I., Pessenda, L.C.R., Fontes, N.A., Cohen, M.C. L., et al., 2020. An integrated analysis of palynofacies and diatoms in the Jucuruçu river valley, northeastern Brazil: holocene paleoenvironmental changes. *J. S. Am. Earth Sci.* 103, 102731. <https://doi.org/10.1016/j.jsames.2020.102731>.
- Mann, T., Serwa, A., Rovere, A., Casella, E., Appeaning-Addo, K., Jayson-Quashigah, P. N., Mensah-Seno, T., Trstenjak, K., Lassalle, B., Flitner, M., Westphal, H., 2023. Multi-decadal shoreline changes in Eastern Ghana—Natural dynamics versus human interventions. *Geo Mar. Lett.* 43 (17). <https://doi.org/10.1007/s00367-023-00758-x>.
- Martin, L., Bittencourt, A.C.S.P., Vilas Boas, G.S., Flexor, J.M., 1980. Mapa geológico do quaternário costeiro do estado da Bahia – 1:250.000. In: Secretaria das Minas e energia/Coordenação de Produção Mineral, vol. 60. Salvador.
- Martin, L., Dominguez, J.M.L., Abilio, C.S.P., Bittencourt, A.C.S.P., 2003. Fluctuating Holocene sea levels in eastern and southeastern Brazil: evidence from multiple fossil and geometric indicators. *J. Coast Res.* 19 (1), 101–124.
- Martin, L., Suguio, K., Flexor, J.M., 1993. As flutuações de nível do mar durante o quaternário superior e a evolução geológica de “deltas” brasileiros. *Bol. IG-USP Publicacão Espec.* 15 (15), 184. <https://doi.org/10.11606/issn.2317-8078.v0i15p01-186>.
- Martinez, P., Suguio, K., Lopez-Mazzetto, J.M., Gianinni, P.C.F., Schellekens, J., Vidal-Torrado, P., 2018. Geomorphological control on podzolisation - an example from a tropical barrier island. *Geomorphology* 309, 86–97. <https://doi.org/10.1016/j.geomorph.2018.02.030>.
- Martins, D.C., Cancelli, R.R., Lopes, R.P., Testa, P.H.E., Barboza, E.G., 2018. Ocorrência de Ophiomorpha Nodosata em sedimentos Pleistocénicos da planície costeira da pinheira, Santa Catarina. Brasil. *Revista Brasileira de Paleontologia* 21 (1), 79–86. <https://doi.org/10.4072/rbp.2018.1.06>.
- Martins, L.R., 2003. Recent sediments and grain-size analysis. *Gravel* 1, 90–105.
- Martins, S.E.M., França, M.C., Seddique, A.A., Sial, A.N., Pessenda, L.C.R., Camargo, P.B., Valença, L.M.M., Santos, L.R.O.C., Barcellos, R.L., 2021. Holocene vegetation changes according to sea-level and climate dynamics on tidal flats of the Formoso river estuary, northeastern Brazil. *Quat. Int.* 602, 39–48. <https://doi.org/10.1016/j.quaint.2020.07.032>.
- Masselink, G., Hughes, M., Knight, J., 2011. Introduction to Coastal Processes and Geomorphology, second ed. Routledge. <https://doi.org/10.4324/9780203785461>.
- Mesciolotti, P.C., Pupim, F.N., Ladeira, F.S.B., Sawakuchi, A.O., Catharina, A.S., Assine, M.L., 2021. Fluvial aggradation and incision in the Brazilian tropical semi-arid: climate-controlled landscape evolution of the São Francisco river. *Quat. Sci. Rev.* 263, 106–977. <https://doi.org/10.1016/j.quascirev.2021.106977>.
- Miali, A.D., 1996. The geology of fluvial deposits (sedimentary facies. Basin Analysis, and Petroleum Geology). Springer, p. 565.
- Monteiro, H.S., Vasconcelos, P.M., Farley, K.A., Mello, C.L., Conceição, F.T., 2022. Long-term vegetation-induced goethite and hematite dissolution-reprecipitation along the Brazilian Atlantic margin. *Palaeogeogr. Palaeoclimatol. Palaeoecol.* 601, 111137. <https://doi.org/10.1016/j.palaeo.2022.111137>.
- Moreira, V.B., Lämmle, L., Torres, B.A., Ayer, J.E.B., Mincato, R.L., 2022. Gênese e distribuição espacial de Espodossolos no Brasil: uma revisão sob o viés micromorfológico. *InterEspaço: Revista de Geografia e Interdisciplinaridade* 8, e202202. <https://doi.org/10.18764/2446-6549.e202202>.
- Moreira, V.B., 2021. Geocronologia de coberturas Superficiais em baixos terraços na foz dos rios Una/Pardo (BA), relacionados a transgressões e regressões marinhas decorrentes de pulsações climáticas holocênicas. 203p. Tese (doutorado) – Universidade Estadual de Campinas, vol. 203p. Instituto de Geociências.
- Moreira, V.B., Lämmle, L., Torres, B.A., Donadio, C., Perez Filho, A., 2024. Geomorphological evolution in transitional environments on the eastern coast of Brazil. *Earth Surf. Process. Landf.* 49 (14), 4679–4693. <https://doi.org/10.1002/esp.5989>.
- Murray, A., Wintle, A.G., 2000. Luminescence dating of quartz using an improved single-aliquot regenerative-dose protocol. *Radiat. Meas.* 32, 57–73. [https://doi.org/10.1016/S1350-4487\(99\)00253-X](https://doi.org/10.1016/S1350-4487(99)00253-X).
- Murray, A., Wintle, A.G., 2003. The single aliquot regenerative dose protocol: potential for improvements in reliability. *Radiat. Meas.* 37 (4–5), 377–381. [https://doi.org/10.1016/S1350-4487\(03\)00053-2](https://doi.org/10.1016/S1350-4487(03)00053-2).
- Nascimento, L., Bittencourt, A., N. S., Santos, A.N., Dominguez, J.M.L., 2007. Deriva litorânea ao longo da costa do caucá, Bahia: repercussões em geomorfologia costeira. *Revista Pesquisa em Geociências* 34 (2), 45–56. <https://doi.org/10.22456/1807-9806.19471>.
- Nelson, M.S., Gray, H.J., Johnson, J.A., Rittenour, T.M., Feathers, J.K., Mahan, S.A., 2015. User guide for luminescence sampling in archaeological and geological contexts. *Adv. Archaeol. Practice: A J. Soc. Am. Archaeol.* 3 (2), 166–177. <https://doi.org/10.7183/2326-3768.3.2.166>.
- Novello, V.F., Cruz, F.W., Moquet, J.S., Vuille, M., de Paula, M.S., Nunes, D., et al., 2018. Two millennia of South Atlantic convergence zone variability reconstructed from isotopic proxies. *Geophys. Res. Lett.* 45 (10), 5045–5051. <https://doi.org/10.1029/2017GL076838>.
- Pennetta, M., Brancato, V.M., De Muro, S., Gioia, D., Kalb, C., Stanislao, C., Valente, A., Donadio, C., 2016. Morpho-sedimentary features and sediment transport model of the submerged beach of the ‘Pineta della foce del Garigliano’ SCI Site (Caserta, southern Italy). *J. Maps* 12 (1), 139–146. <https://doi.org/10.1080/17445647.2016.1171804>.
- Perez Filho, A., Moreira, V.B., Lämmle, L., Souza, A.O., Torres, B.A., Aderaldo, P.I.C., Valezio, É.V., Machado, D.O.B.F., Prebianca, M.M., Mazoni, A.F., Zabini, C.,

- Rubira, F.G., 2022. Genesis and distribution of low fluvial terraces formed by Holocene climate pulses in Brazil. *Water* 14, 2977. <https://doi.org/10.3390/w14192977>.
- Rasmussen, S.O., Bigler, M., Blockley, S.P., et al., 2014. A stratigraphic framework for abrupt climatic changes during the Last Glacial period based on three synchronized Greenland ice-core records: refining and extending the INTIMATE event stratigraphy. *Quat. Sci. Rev.* 106, 14–28. <https://doi.org/10.1016/j.quascirev.2014.09.007>.
- Rhodes, E.J., 2011. Optically stimulated luminescence dating of sediments over the past 200,000 years. *Annu. Rev. Earth Planet Sci.* 39 (1), 461–488. <https://doi.org/10.1146/annurev-earth-040610-133425>.
- Ribeiro, S.R., Valadão, R.C., Gomes, M.O.S.G., Bittencourt, J.S.B., Alves, R.A., 2023. Paleoecological indicators of the highstand sea level on the Amazonian supralittoral until the last two millennia. *J. S. Am. Earth Sci.* 128, 104422. <https://doi.org/10.1016/j.jsames.2023.104422>.
- Rodrigues, J.M., Behling, H., Giesecke, T., 2016. Holocene dynamics of vegetation change in southern and southeastern Brazil is consistent with climate forcing. *Quat. Sci. Rev.* 146, 54–65, 2016.
- Rossi, M., Queiroz Neto, J.P., Bras, R., 2021. Os solos como indicadores das relações entre sedimentos continentais e marinhos na planície costeira: rio Guaratuba (SP). *Ci. Solo. Vigosa* 25, 113–120. <https://doi.org/10.1590/S0100-06832001000100012>.
- Rovere, A., Pico, T., Richards, F., O'Leary, M.J., Mitrovica, J.X., Goodwin, I.D., Austermann, J., Latychev, K., 2023. Influence of reef isostasy, dynamic topography, and glacial isostatic adjustment on sea-level records in Northeastern Australia. *Commun. Earth Environ.* 4, 328. <https://doi.org/10.1038/s43247-023-00967-3>.
- Schubel, J.R., 1971. The estuarine environment: estuaries and estuarine sedimentation. Washington. DC (Diabetol. Croat.): Am. Geol. Inst. Short Course Lecture Notes, 324pp.
- Silveira, J.D., 1952. Baixadas litorâneas quentes e úmidas. *Boletim da FFCL da USP. Geografia* n° 8, 241.
- Souza, A.O., Perez Filho, A., Arruda, E.M., Cerreto, C., Lämmle, L., 2024. Fluvial responses to Holocene climatically induced coastline migration in the Iguape river estuary (Southeast Brazil). *Earth Surf. Process. Landf.* 49 (14), 4694–4708. <https://doi.org/10.1002/esp.5990>.
- Stríkis, N.M., Cruz, F.W., Cheng, H., Karmann, I., Edwards, R.L., Vuille, M., Wang, X., Paula, M.S., Novello, V.F., Auler, A.S., 2011. Abrupt variations in South American monsoon rainfall during the Holocene based on a speleothem record from central-eastern Brazil. *Geology* 39, 1075–1078. <https://doi.org/10.1130/G32098.1>.
- Suguió, K., Martin, L., Bittencourt, A.C.S.P., Dominguez, J.M.L., Flexor, J.M., Azevedo, A. E.G., 1985. Flutuações do nível relativo do mar durante o Quaternário superior ao longo do litoral brasileiro e suas implicações na sedimentação costeira. *Rev. Bras. Geociências* 15, 273–286. <https://doi.org/10.25249/0375-7536.1985273286>.
- Suguió, K., 2010. *Geologia do Quaternário e mudanças ambientais*, second ed. Oficina de Textos, São Paulo, p. 408p.
- Tomazelli, L.J., Dillenburg, S.R., 2007. Sedimentary facies and stratigraphy of a last interglacial coastal barrier in south Brazil. *Mar. Geol.* 244, 33–45. <https://doi.org/10.1016/j.margeo.2007.06.002>.
- Tricart, J., 1958. Notas sobre variação quaternária do nível marinho. *Boletim Paulista de Geografia*. N° 28, 3–13.
- Wintle, A.G., Murray, A.S., 2006. A review of quartz optically stimulated luminescence characteristics and their relevance in single-aliquot regeneration dating protocols. *Radiat. Meas.* 41 (1), 369–391. <https://doi.org/10.1016/j.radmeas.2005.11.001>.